T. Mizoguchi *et al.*, "High Accurate Representation of Turn-on Switching Characteristics by New IGBT and FWD Compact Models for High Power Applications," *2020 32nd International Symposium on Power Semiconductor Devices and ICs (ISPSD), Vienna, Austria, 2020*, pp. 478-481, doi: 10.1109/ISPSD46842.2020.9180189

High Accurate Representation of Turn-on Switching Characteristics by New IGBT and FWD Compact Models for High Power Applications

Takeshi Mizoguchi, Yoshiko Ikeda, and Naoto Tsukamoto
Toshiba Electronic Devices & Storage Corporation, Saiwai-Ku, Kawasaki 212-8520, Japan
Email: takeshi3.mizoguchi@glb.toshiba.co.jp

***Abstract*—In this paper, we report a newly developed the insulated gate bipolar transistor (IGBT) and the free-wheeling diode (FWD) compact models considered with bipolar carrier dynamics for prediction of power-loss and Electro-Magnetic-Interference (EMI) noise accurately. The capabilities of the proposed IGBT and FWD models considered with carrier dynamics are demonstrated by reproduction of the measured turn-on switching waveform for multiple external gate resistance (R_g) values. In addition, it is also demonstrated that the proposed models can be successfully utilized for different collector currents and temperature conditions with high convergence.**

***Keywords*—IGBT, FWD, compact model, MBD, circuit simulation.**

I. Introduction

Power semiconductor devices are utilized for various inverter and converter circuits for power applications and are essential for power switching, converter, motor control, and so on [1]. Recently, a model-based-design (MBD) is focused on automotive and power electronics system design for virtual prototyping. In order to accurately predict circuit losses and EMI noise, compact model is a powerful tool for the power electronics design and its accuracy has been improved continuously.

For high power applications, the IGBT is one of the most important power semiconductor device which integrate MOS-gate control with bipolar conductivity modulation to achieve high input impedance and low on-resistance. The bipolar action originates the complex switching performance, although the conduction loss can be reduced. For an example, the tail current is shown during the turn-off switching because of the remove of the stored carriers in the drift region [2]. Numerous works on IGBT compact models have been reported [3]–[8]. Although the model of bipolar devices, such as IGBT and FWD devices, has been studied, the representation of switching waveform is not sufficient for the MBD process due to complicated bipolar actions. In particular, IGBT turn-on characteristics greatly affect both power-loss and EMI noise, and depend on the accuracy of both IGBT and FWD compact models. In addition, the convergence in a simulation is also problematic for the MBD process. This paper reports the new IGBT and FWD compact models considered with bipolar carrier dynamics with high convergence. The simulation results using the proposed compact models show high accurate turn-on characteristics even for various operating conditions.

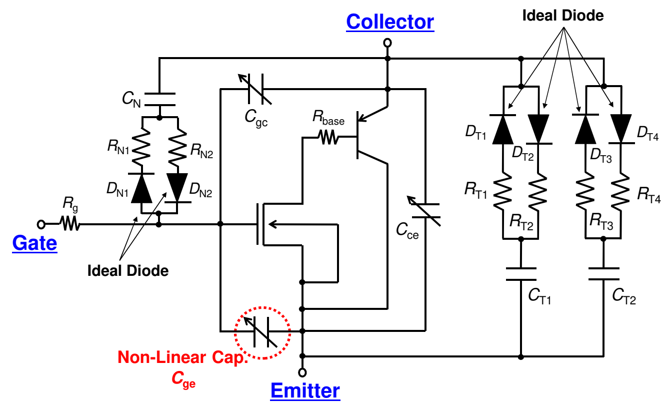

Fig. 1. Proposed model structure of IGBT devices. The proposed IGBT model consists of a MOSFET part, a bipolar part, C_{ge} formed by non-linear functions and the sub-circuits with ideal-diode connected to the gate-collector and the collector-emitter.

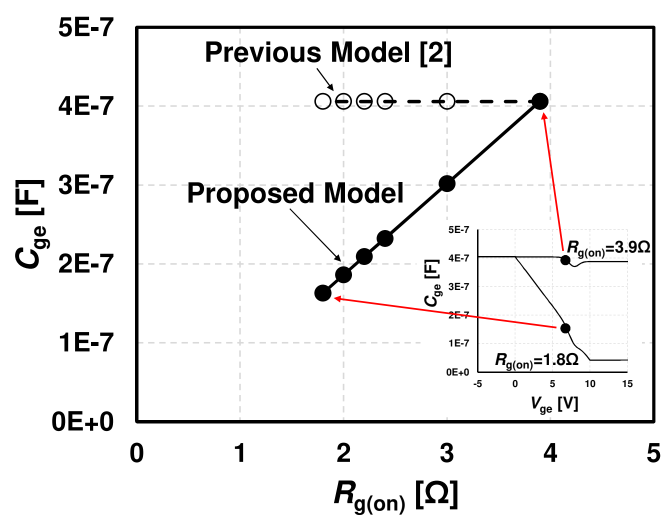

Fig. 2. Comparison of an external gate resistance for the turn-on switching operation $R_{\mathrm{g(on)}}$ dependency of modeled C_{ge} at V_{ce}=1000V, V_{ge}=7V with proposed and previous models and C_{ge}-V_{ge} characteristics at V_{ce}=1000V and $R_{\mathrm{g(on)}}$=1.8Ω, 3.9Ω with the proposed model.

II. Model Descriptions

A. IGBT model

Fig. 1 shows the proposed model structure of IGBT devices in this work. Similarly to our previous work [2], the proposed model consists of a MOSFET part and a bipolar part. The proposed model has two specific features. One is the C_{ge}

formed by non-linear functions which consider the negative capacitance [9] for reproducing the turn-on $\mathrm{d}I/\mathrm{d}t$. Another feature is sub-circuits with ideal-diode and CR connected to the gate-collector and the collector-emitter for reproducing the turn-off $\mathrm{d}V/\mathrm{d}t$ and the tail current. The sub-circuit connected to gate-collector represents the effective C_{gc} during the turn-off switching and adjusts the turn-off $\mathrm{d}V/\mathrm{d}t$. Moreover two parallel sub-circuits connected to the collector-emitter represents the tail current due to these different time-constant values of the sub-circuits.

In the power electronics system design, the switching speed is adjusted by an external gate resistance R_{g} due to the trade-off between power-loss and EMI noise. Therefore, the R_{g} dependency in switching characteristics is one of the most important factor in the IGBT model. For turn-on switching characteristics, the influence of a negative gate capacitance upon C_{ge} must be considered in the IGBT model. Fig. 2 shows the C_{ge} as a function of an external gate resistance for the turn-on switching operation $R_{\mathrm{g(on)}}$ with fixed V_{ce}=1000V and V_{ge}=7V. Even though the negative gate capacitance is enhanced at high speed switching (small $R_{\mathrm{g(on)}}$ condition) due to increase of hole around the gate, the $R_{\mathrm{g(on)}}$ dependency of the C_{ge} is extremely small by our previous model. Therefore, the $R_{\mathrm{g(on)}}$ dependency of the C_{ge} has been considered in the proposed IGBT model.

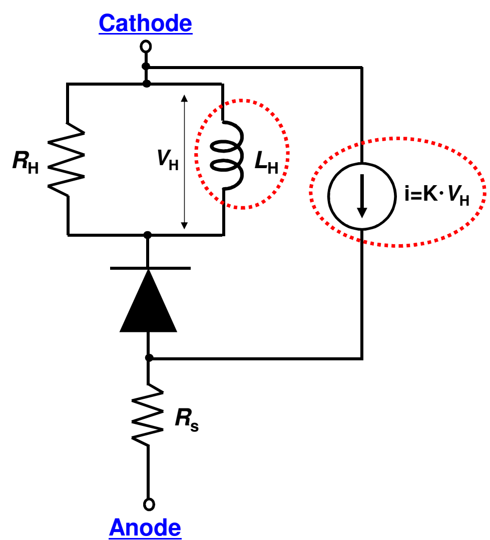

Fig. 3. Proposed model structure of FWD devices. K and L_{H} are model parameters for the reverse recovery characteristic.

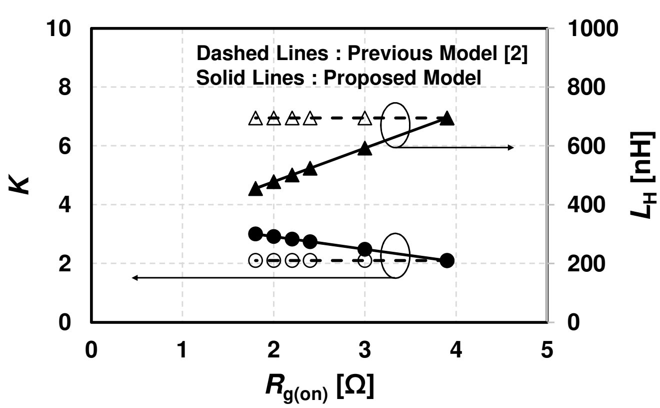

Fig. 4. Comparison of $R_{\mathrm{g(on)}}$ dependency of modeled the voltage-controlled current source parameter K and the inductor L_{H} with previous and proposed models.

B. FWD model

Fig. 3 shows the proposed model structure of FWD devices in this work. The proposed model consists of a standard diode, two resistances, an inductance and a voltage-controlled current source. The surge current during the turn-on switching is determined by the FWD reverse recovery characteristics, which are represented by the voltage-controlled current source and inductor L_{H} in the FWD model [10].

Fig. 4 shows the modeled voltage-controlled current source parameter K and the inductor L_{H} as a function of an external gate resistance for the turn-on switching operation $R_{\mathrm{g(on)}}$. The recovery characteristics depend on the turn-on switching time, because the reverse recovery current I_{rr} and the reverse recovery time T_{rr} are influenced by the carrier recombination during the switching due to the carrier lifetime. Therefore, the $R_{\mathrm{g(on)}}$ dependency of the voltage-controlled current source parameter K and L_{H} have been added in the proposed FWD model in order to representation of the I_{rr} and T_{rr} during the switching operation.

III. Circuit Simulation Results and Discussions

To analyze the switching characteristics, the model parameters of the proposed models were extracted from 4.5kV/3000A IEGT (Toshiba ST3000GXH31A)

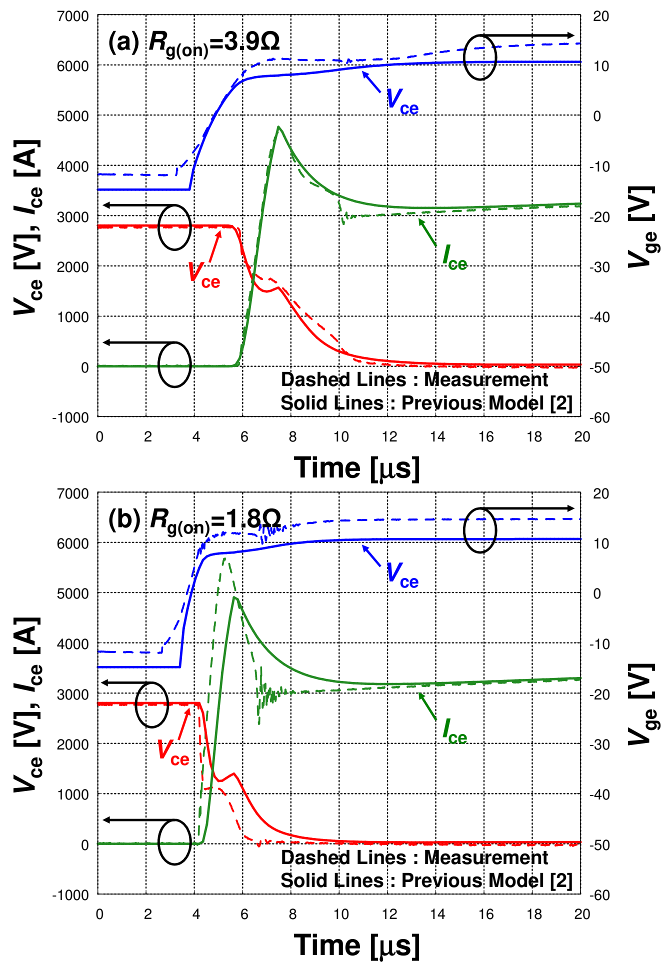

Fig. 5. Comparison of the measured and the simulated turn-on switching waveforms with the previous model (a) $R_{\mathrm{g(on)}}$=3.9Ω, (b) $R_{\mathrm{g(on)}}$=1.8Ω at the room temperature with consideration of parasitic components of the studied inductive load switching circuit.

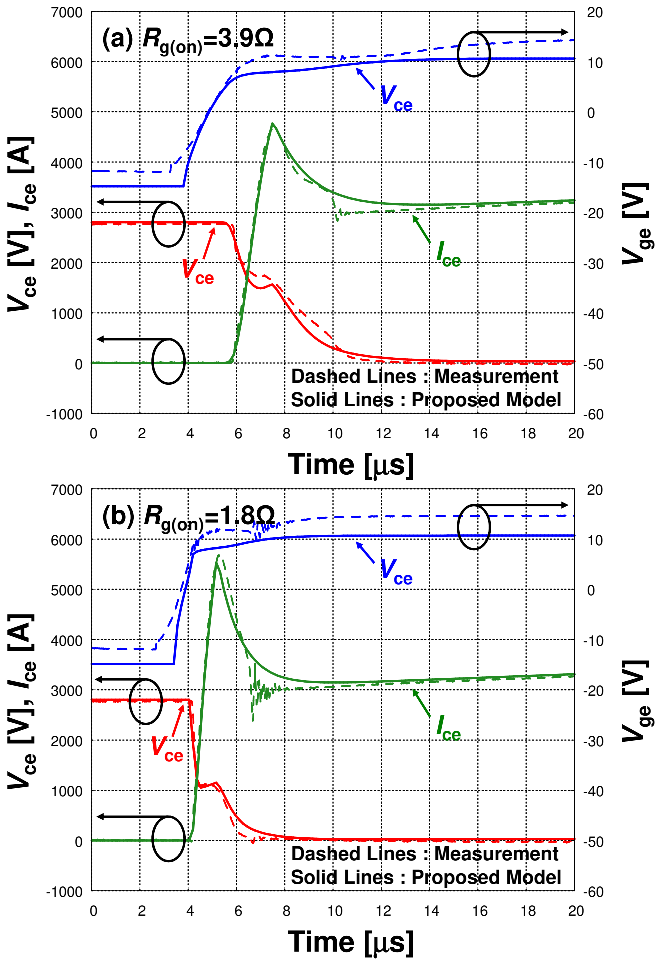

Fig. 6. Comparison of the measured and the simulated turn-on switching waveforms with the proposed model (a) $R_{g(on)}$=3.9Ω, (b) $R_{g(on)}$=1.8Ω at the room temperature with consideration of parasitic components of the studied inductive load switching circuit.

and 4.5kV/3000A fast recovery diode (FRD) (Toshiba 3000GXHH28) characteristics, respectively. The model accuracy was evaluated by the inductive load switching characteristics (Input voltage V_{in}=±15V, Supply voltage V_{cc}=2800V and Load inductor L_{load}=150μH) considering with the parasitic components in the measurement circuit.

A. Turn-on switching characteristics

Figs. 5(a) and (b) shows a comparison of the measured and the simulated turn-on switching waveforms by the previous model. At small $R_{g(on)}$=1.8Ω, a hump of V_{ge} is clearly shown due to the enhancement of the negative gate capacitance. Since the previous model employs a constant negative gate capacitance, the difference of current waveform between the simulation and the measurement is clearly shown at small $R_{g(on)}$=1.8Ω as shown in Fig. 5(b).

On the other hand, the proposed model obtains to represent the measured turn-on switching waveform by the $R_{g(on)}$ dependency of the C_{ge} in the IGBT model, voltage-controlled current source parameter K and the inductor L_H in the FWD model. Figs. 6(a) and (b) shows a comparison of the measured and the simulated turn-on switching waveforms by the proposed models. Even at the low $R_{g(on)}$ condition, the proposed models achieves high representation of the measured turn-on switching waveform as shown in Fig. 6(b).

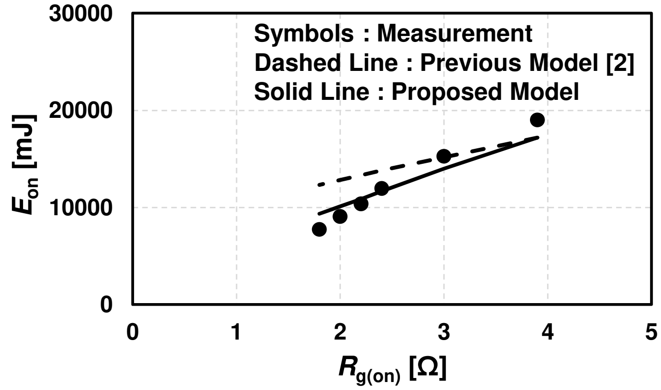

Fig. 7. Comparison of measured and simulated $R_{g(on)}$ dependency of the turn-on loss E_{on} with previous and proposed models at room temperature.

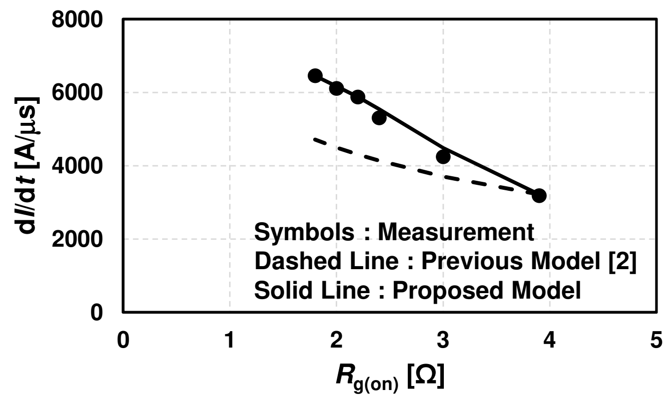

Fig. 8. Comparison of measured and simulated $R_{g(on)}$ dependency of turn-on dI/dt with previous and proposed models at room temperature.

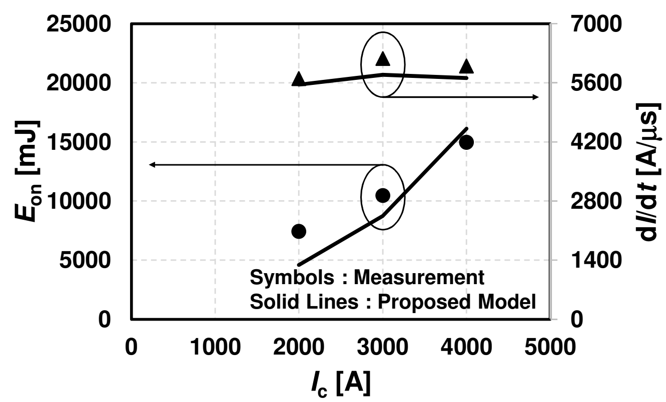

Fig. 9. Comparison of measured and simulated collector current I_c dependency of turn-on loss E_{on} and dI/dt with proposed model at room temperature.

Since the proposed model gives priority to the representation E_{on} and dI/dt, the representation of V_{ge} waveform is not sufficient. The offset of V_{ge} waveform between the simulation and measurement is caused by the difference of the gate input signal configuration and the parasitic gate inductance. Fig. 7 shows a comparison of measured and simulated $R_{g(on)}$ dependency of the turn-on loss E_{on} with previous and proposed models at room temperature. As a result, the error of the E_{on} is decreased from 37% to 17% by the proposed model at $R_{g(on)}$=1.8Ω. Fig. 8 shows a comparison of measured and simulated $R_{g(on)}$ dependency of the turn-on dI/dt with previous and proposed models at room temperature.

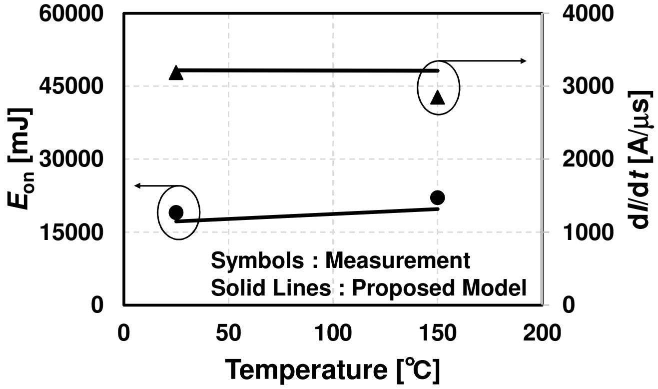

Fig. 10. Comparison of measured and simulated temperature dependency of the turn-on loss $E_{\rm on}$ and the turn-on dI/dt with proposed model at $R_{\rm g(on)}$=3.9Ω and $I_{\rm c}$=3000A.

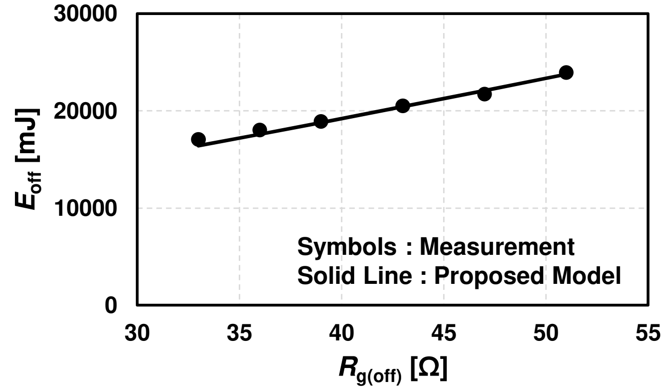

Fig. 11. Comparison of measured and simulated $R_{\rm g(off)}$ dependency of the turn-off loss $E_{\rm off}$ with the proposed models at room temperature.

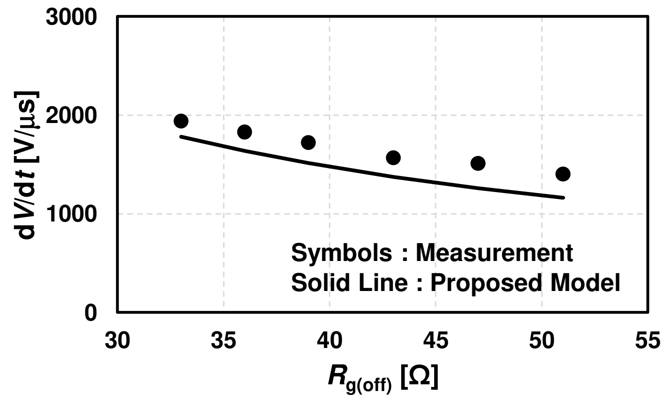

Fig. 12. Comparison of measured and simulated $R_{\rm g(off)}$ dependency of turn-off dV/dt with the proposed models at room temperature.

The error of the turn-on dI/dt is also decreased from 37% to almost 0% at $R_{\rm g(on)}$=1.8Ω. Even when collector current and temperature conditions have been changed, the reproducibility of the proposed models have been kept as shown in Fig. 9 and Fig. 10. The errors of the turn-on loss $E_{\rm on}$ and the turn-on dI/dt are less than 25% and 8%, respectively.

B. Turn-off switching characteristics

In the proposed model, accuracy of the turn-off characteristics is maintained from the previous model [2]. Fig. 11 and Fig. 12 shows a comparison of measured and simulated external gate resistance for the turn-off switching operation $R_{\rm g(off)}$ dependency of the turn-off loss $E_{\rm off}$ and the turn-off dV/dt with the proposed model, respectively. For multiple $R_{\rm g(off)}$ values, the turn-off loss $E_{\rm off}$ and the turn-off dV/dt are also reproduced accurately.

Since the proposed models are composed only with some simple devices, good convergence is also achieved. The simulation time for 1 cycle of double plus switching (turn-off and turn-on) operation using the proposed models is only less than 1s as same as that of the previous model [2]. Consequently, it is concluded that the proposed models don't sacrifice the simulation time for high accurate representation of power-loss and EMI noise.

IV. Conclusion

We have developed the newly compact model for IGBT and FWD devices considered with bipolar carrier dynamics into several model parameters. The proposed models successfully reproduce the measured turn-on switching characteristics for various operating conditions. Furthermore, the turn-off switching simulation results are in good agreement with the measurement results for multiple external gate resistance values. From these results, the proposed IGBT and FWD compact models are useful for high accurate prediction of both the power-loss but also EMI noise for the MBD process.

Acknowledgment

The authors would like to thank Prof. Wataru Saito of Kyushu University for giving valuable advices and the continuous technical support of this work.

References

[1] T. Mizoguchi. T. Naka, Y. Tanimoto, Y. Okada, W. Saito, M. Miura-Mattausch, and H. J. Mattausch, "Analysis of GaN-HEMT Switching Characteristics for High-Power Applications", Proc. the 28$^{\rm th}$ ISPSD, pp. 267–270, 2016.

[2] T. Mizoguchi. Y. Sakiyama, N. Tsukamoto, and W. Saito, "High Accurate IGBT/IEGT Compact Modeling for Prediction of Power Efficiency and EMI Noise", Proc. the 31$^{\rm st}$ ISPSD, pp. 307–310, 2019.

[3] Z. Shen, and T. P. Chow, "An Analytical IGBT Model for Power Circuit Simulation", Proc. the 3$^{\rm rd}$ ISPSD, pp. 79–82, 1991.

[4] Z. Shen, and T. P. Chow, "Modeling and Characterization of the Insulated Gate Bipolar Transistor (IGBT) for SPICE Simulation", Proc. the 5$^{\rm th}$ ISPSD, pp. 79–82, 1991.

[5] R. Kraus, P. Türkes, J. Sigg, "Physic-Based Models of Power Semiconductor Devices for the Circuit Simulator SPICE", 29$^{\rm th}$ Annual Power Electronics Specialists Conference, pp.1726–1731, 1998.

[6] R. Azar, F. Udrea, M. De Silva, G. Amaratunga, W. T. Ng, F. Dawson, W. Findlay, and P. Waind, "Advanced SPICE Modeling of Large Power IGBT Modules", 37$^{\rm th}$ IAS Annual Meeting, vol. 4, pp. 2433–2436, 2002.

[7] R. Azar, F. Udrea, W. T. Ng, F. Dawson, W. Findlay, P. Waind, and G. Amaratunga, "Advanced Elecrto-thermal SPICE Modeling of Large Power IGBTs", Proc. the 15$^{\rm th}$ ISPSD, pp. 291–294, 2003.

[8] D. Navarro, T. Sano, and Y. Furui, "A Sequential Model Parameter Extraction Technique for Physcal-Based IGBT Compact Models", IEEE Trans. Electron Devices, vol. 60, no. 2, pp. 580–586, 2013.

[9] M. Yamaguchi, I. Omura, S. Urano, S. Umekawa, M. Tanaka, T. Okuno, T. Tsunoda, and T. Ogura, "IEGT Design Criterion for Reducing EMI Noise", Proc. the 16$^{\rm th}$ ISPSD, pp. 115–118, 2004.

[10] A. Dastfan, "A New Macro-Model for Power Diodes Reverse Recovery", Proc. the 7$^{\rm th}$ WSEAS International Conference on Power Systems, pp. 15–17, 2007.